

CYFIP/Sra-1 Controls Neuronal Connectivity in *Drosophila* and Links the Rac1 GTPase Pathway to the Fragile X Protein

Annette Schenck,^{1,2} Barbara Bardoni,^{1,*}
Caillin Langmann,³ Nicholas Harden,³
Jean-Louis Mandel,¹ and Angela Giangrande^{2,*}

¹Department of Molecular Pathology

²Department of Developmental Biology

Institut de Génétique et de Biologie

Moléculaire et Cellulaire

CNRS/INSERM/ULP, Boite Postale 10142

67404 Illkirch Cedex

France

³Department of Molecular Biology
and Biochemistry

Simon Fraser University

8888 University Drive

Burnaby, British Columbia, V5A 1S6

Canada

Summary

Neuronal plasticity requires actin cytoskeleton remodeling and local protein translation in response to extracellular signals. Rho GTPase pathways control actin reorganization, while the fragile X mental retardation protein (FMRP) regulates the synthesis of specific proteins. Mutations affecting either pathway produce neuronal connectivity defects in model organisms and mental retardation in humans. We show that CYFIP, the fly ortholog of vertebrate FMRP interactors CYFIP1 and CYFIP2, is specifically expressed in the nervous system. CYFIP mutations affect axons and synapses, much like mutations in *dFMR1* (the *Drosophila* FMR1 ortholog) and in Rho GTPase *dRac1*. CYFIP interacts biochemically and genetically with *dFMR1* and *dRac1*. Finally, CYFIP acts as a *dRac1* effector that antagonizes FMR1 function, providing a bridge between signal-dependent cytoskeleton remodeling and translation.

Introduction

Understanding the molecular mechanisms involved in neuronal wiring and in activity-dependent plasticity is one of the most important topics of modern neurobiology, since these processes control cognitive functions. Analysis of model organisms and genes mutated in cases of inherited mental retardation has identified two types of molecules important for such processes, the fragile X mental retardation protein (FMRP) and Rho GTPases (reviewed in Bardoni and Mandel, 2002; Ramakers, 2002; Chelly and Mandel, 2001). Rho GTPase pathways remodel actin cytoskeleton in response to extracellular stimuli (Hall, 1998). In neurons, they regulate axon and dendrite outgrowth as well as development, maturation, and maintenance of dendritic spines,

the postsynaptic site of most excitatory synapses in mammalian brains (for review see Luo, 2002).

Fragile X syndrome, the most frequent cause of hereditary mental retardation, is caused by the absence of the RNA binding protein FMRP (for review see Bardoni et al., 2001). FMRP is present at synapses and can act as a translational regulator (Weiler et al., 1997; Lagerbauer et al., 2001; Li et al., 2001; Brown et al., 2001; Miyashiro et al., 2003; Zalfa et al., 2003). It binds to specific mRNAs through an RNA G quartet structure (Schaeffer et al., 2001; Darnell et al., 2001), and its *Drosophila* ortholog, *dFMR1*, has been recently found to associate with the RNAi silencing machinery (Ishizuka et al., 2002; Caudy et al., 2002). Misregulation of target mRNAs may account for the abnormal maturation of dendritic spines that has been observed in brains of fragile X patients and in knockout mice (Comery et al., 1997; Irwin et al., 2000; Nimchinsky et al., 2001).

Whether and how the molecular pathways controlling translation and cytoskeleton remodeling are connected is not yet understood. Our approach to identify FMRP interacting proteins (Bardoni et al., 1999) has recently led to the characterization of the human cytoplasmic FMRP interacting proteins CYFIP1 and CYFIP2, which are 88% identical in their amino acid sequence (Schenck et al., 2001). CYFIP1, also known as Sra-1, had been previously described as an interactor of Rac1 (Kobayashi et al., 1998), a Rho GTPase family member. Hence, the identification of the CYFIP1 and CYFIP2 suggested a direct connection between signaling pathways controlling neuronal plasticity and cognition.

The *Drosophila* genome contains a single ortholog of the human FXR gene family (coding for FMRP and its related proteins FXR1P and FXR2P): *dFMR1* (also called *dFXR*). *dFMR1*'s biochemical properties and role seem conserved in the fly nervous system (Wan et al., 2000; Zhang et al., 2001; Morales et al., 2002; Dockendorff et al., 2002; Schenck et al., 2002). A single fly CYFIP gene (Schenck et al., 2001) is similarly related to human CYFIP1 and CYFIP2 (67% identity at the protein level). Finally, the GTPase *dRac1* has been extensively studied in flies. The existence of single FXR and CYFIP orthologs as well as the evolutionary functional conservation makes the fly an ideal model to elucidate their role in neuronal morphogenesis and plasticity in vivo.

We show here that *Drosophila* CYFIP/Sra-1, which we will refer to as "CYFIP" throughout the text, is highly expressed in neurons, where it accumulates in central axons and at motor neuron terminals. CYFIP mutations are lethal and induce defects in axon growth, branching, and pathfinding. The overall organization of the neuromuscular junction (NMJ) is also significantly affected. Loss of CYFIP therefore involves defects that have been previously described in *dFMR1* and/or *dRac1* mutants (Morales et al., 2002; Dockendorff et al., 2002; Luo et al., 1994; Hakeda-Suzuki et al., 2002). We provide evidence for CYFIP-*dFMR1* and CYFIP-*dRac1* biochemical interactions. Finally, dosage-dependent experiments reveal genetic interactions in vivo. These latter experiments allow us to order the three molecules within a

*Correspondence: angela@titus.u-strasbg.fr (A.G.), bardoni@titus.u-strasbg.fr (B.B.)

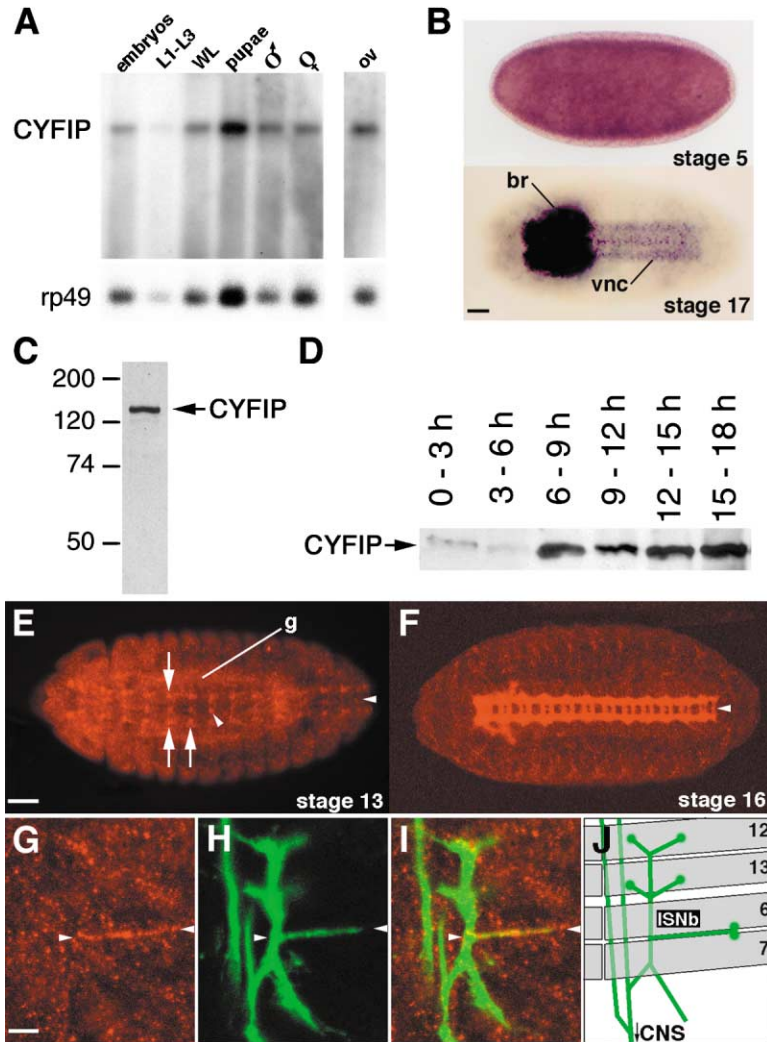


Figure 1. CYFIP Profile of Expression

(A) Northern blot analysis throughout development. Lanes correspond to poly(A)⁺ RNA isolated from pooled embryonic (embryos) or larval (L1–L3) stages, from wandering larvae (WL), pupae, adult males or females. “ov” indicates mRNA isolated from dissected adult ovaries. The same blot was probed with a loading control (rp49, lower panel).

(B) In situ hybridization on whole-mount embryos, anterior to the left. *CYFIP* mRNA is uniformly distributed at early embryonic stages (stage 5) and predominantly expressed in the central nervous system (CNS) at stage 17 (dorsal view). br, brain; vnc, ventral nerve cord.

(C) Western blot analysis of *Drosophila* S2 cell line extract using anti-CYFIP.

(D) Western blot analysis of staged embryos. Equivalent amounts of protein extracts were loaded. Embryonic stages are indicated at the top as hours after egg laying at 25°C.

(E and F) *CYFIP* immunolabeling of whole-mount embryos at stage 13 and 16, respectively, ventral views. (E) CNS (arrows), midline (arrowheads), and gut (g) labeling. (F) *CYFIP* strongly accumulates in CNS axons. Moderate labeling is also present in some peripheral structures.

(G–I) Stage 17 embryo double labeled with anti-Fas II (green) and anti-CYFIP (red) to visualize axon terminals of intersegmental motor nerve b (ISNb) at the muscle 6/7 junction (arrowheads). Dorsal is up, anterior to the left. Pictures represent projections of three confocal sections at the focal plane of the muscle 6/7 junction.

(J) Schematic representation of lateral muscles and innervation pattern by ISNb.

Scale bars, 50 μm (B, E, and F), 5 μm (G–J).

pathway that regulates neuronal morphology and connectivity.

Results

Cloning of *CYFIP* and Expression Profile throughout Development

A full-length *Drosophila CYFIP* cDNA (accession number AY017343; Schenck et al., 2001) was obtained by using two overlapping EST clones. To assess at which stage *CYFIP* is expressed, we performed Northern blot analysis on poly(A)⁺ RNA from embryos, larvae, wandering larvae, pupae, and adults. *CYFIP* is present throughout the fly life cycle as a single transcript of around 4.5 kb and is also abundant in adult ovaries (Figure 1A). Signal quantification and normalization against a loading control indicated that there are no major peaks of *CYFIP* expression at specific stages (Figure 1A). In situ hybridization revealed that *CYFIP* is ubiquitously and highly expressed in embryos at precellular (data not shown) and cellular blastoderm stages (Figure 1B, stage 5). Starting from stage 12, *CYFIP* labeling is mostly detected in the developing central nervous system (CNS) and in the gut. While *CYFIP* labeling in the gut diminishes

as development proceeds, CNS labeling persists and increases in intensity until the end of embryogenesis (data not shown and Figure 1B). In addition, *CYFIP* is expressed at low levels throughout the embryo.

CYFIP Strongly Accumulates in Axons of the CNS

In order to characterize the *CYFIP* protein, we developed an anti-CYFIP antibody, which detects a single band of 145 kD in Western blot analysis on *Drosophila* Schneider (S2) cell and embryonic extracts (Figures 1C and 1D). The size of the recognized protein corresponds to the predicted molecular weight (Schenck et al., 2001). To confirm that this band corresponds to *CYFIP*, we transiently overexpressed the full-length product in S2 cells; extracts of transfected cells contain higher levels of the 145 kD product than nontransfected cells (data not shown).

The *CYFIP* embryonic profile follows that of the transcript. It is detectable by stage 11 in the CNS, by stage 13 in the gut (Figure 1E). Its levels in the CNS increase until the end of embryogenesis (Figure 1F). *CYFIP* is a cytoplasmic protein—like its human orthologs— that specifically accumulates in CNS axons, along commissures and longitudinal connectives. Some *CYFIP* ex-

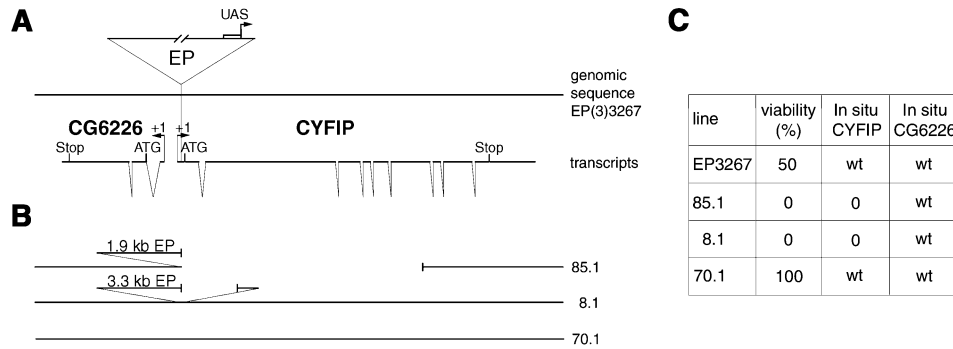


Figure 2. *CYFIP* Locus and Mutants

(A) Organization of the genomic *CYFIP* locus. The *CYFIP* gene is composed of nine coding exons. “EP” indicates the transposon insertion in EP line (3)3267, and “UAS” indicates the upstream activating sequence contained in the transposon. For both *CYFIP* and *CG6226*, the exon/intron organization is shown. “ATG” and “+1” indicate the predicted translation and transcription initiation sites, respectively. “Stop” indicates the end of the predicted open reading frame.

(B) Molecular lesions of some excision mutants.

(C) *CYFIP* and *CG6226* in situ hybridization data on homozygous mutant embryos. The mutant line is indicated in the left column, the utilized probe as well as the viability percentage of homozygous adults in the top row.

pression is detected at the midline (Figures 1E and 1F, arrowheads). Finally, *CYFIP* also accumulates at the motor axon terminals, at the stage at which synaptogenesis is initiated. Double labeling with an antibody (anti-Fas II) recognizing synapses (Schuster et al., 1996) revealed that *CYFIP* is localized at the NMJ (Figures 1G–1J).

Western blot analysis (Figure 1D) shows that *CYFIP* is already present at early embryonic stages (0–3 hr, corresponding to stages 1–6 [according to Campos-Ortega and Hartenstein 1985]), even though its levels are much lower than at later stages (6–18 hr, [stage 12–17]).

Generation of *CYFIP* Null Mutants

The prominent axonal localization suggested a role for the *CYFIP* in axonogenesis. To test this hypothesis, we generated *CYFIP* mutant flies. EP line (3)3267 harbors a transposon on the right arm of the third chromosome, at position 88F. The transposon is inserted within exon 1 of the *CYFIP* gene, in its 5'-UTR (Figure 2A). Southern blotting using an EP-specific probe on genomic DNA isolated from EP(3)3267 and from wild-type (wt) flies confirmed the presence of a single transposon in the EP line (data not shown). EP(3)3267 is a semiviable line, with 50% of the homozygous animals dying before eclosion.

We performed P element mutagenesis and recovered 111 independent excision lines. Eight lines are homozygous lethal and show substantial loss of *CYFIP* immunolabeling. In contrast, all viable or semiviable lines do express *CYFIP*, as assayed in Western blot from homozygous adult extracts (data not shown). Breakpoints were sequenced in three of the eight mutant lines (*CYFIP*^{5.2}, *CYFIP*^{8.1}, *CYFIP*^{85.1}) (Figure 2B and data not shown). We also recovered and characterized three lines (*CYFIP*^{70.1}, *CYFIP*^{1.1}, *CYFIP*^{35.1}) that are 100% viable and constitute precise excision events (Figure 2B and data not shown).

CYFIP is located 250 bp downstream from a gene (*CG6226*) (see Figure 2A) that codes for a putative pepti-

lydisomerase, for which no mutant strain is reported. To assess whether *CYFIP* mutants also affect *CG6226* expression, we performed in situ hybridization using *CYFIP*- and *CG6226*-specific probes on wt, EP(3)3267, and excision lines *CYFIP*^{5.2}, *CYFIP*^{8.1}, *CYFIP*^{85.1}, and *CYFIP*^{70.1} (Figure 2C). While *CYFIP*^{5.2} is null for both genes (data not shown), lines *CYFIP*^{8.1} and *CYFIP*^{85.1} only affect *CYFIP*. Lack of *CYFIP* mRNA in *CYFIP*^{8.1} (EP internal deletion) is likely due to altered stability of the modified transcript. Line *CYFIP*^{85.1}, in which about two-thirds of the *CYFIP* coding region are deleted, was further used to characterize the *CYFIP* null mutant phenotype (Figure 2B) (for loss of *CYFIP* immunoreactivity in this line, see also Figures 5A and 5B).

The analysis of the excision mutants allows us to conclude that loss of *CYFIP* induces lethality, which mostly occurs during pupal life, the first morphological abnormalities being observed around 12 hours after puparium formation. Pupae progressively shrink within the puparium case before the head has everted (data not shown).

CYFIP Is Required for Axonal Pathfinding and Growth

To characterize the effects of *CYFIP* loss, we labeled mutant embryos with antibodies that recognize different subsets and subcellular compartments of neurons in the central and in the peripheral nervous system (CNS and PNS, respectively). The anti-Fas II antibody labels motor axons as well as three central axon fascicles per hemisegment (Figure 3A). A high percentage of *CYFIP* embryos display abnormalities in axon guidance. In 79% of the mutant embryos (n = 150), axons abnormally cross the midline. In most cases, midline crossing occurs once or twice per embryo (Figure 3A', arrow); 13% of the mutants show a more severe phenotype that includes multiple midline crossings (Figure 3A'', arrows), fasciculation defects, and interrupted fascicles (Figure 3A'', arrowheads). Midline crossing was never observed in wt embryos (number of embryos = 100), nor in the precise excision *CYFIP*^{70.1} (n = 150). Central axon label-

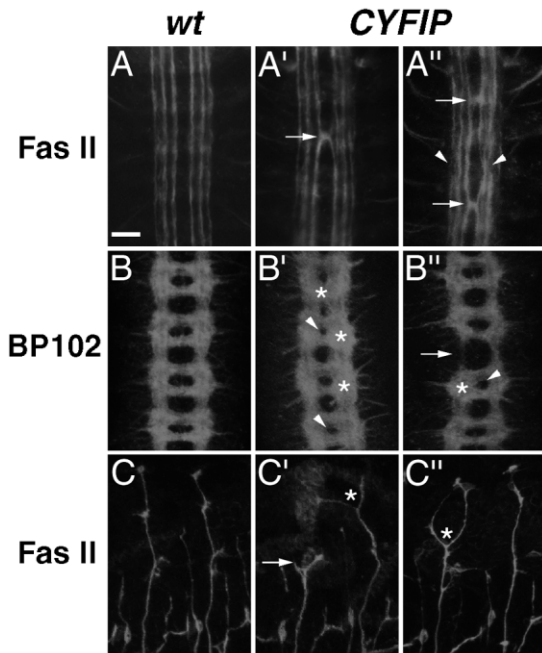


Figure 3. CYFIP Is Required in Central and Peripheral Axons
 Panels (A)–(A'') show Fas II labeling. (A) wt embryo. (A' and A'') *CYFIP*^{85.1} embryos showing midline crossing (arrows). In the most severe case (A''), axons cross the midline several times, and longitudinal connectives are not well separated (arrowheads). Panels (B)–(B'') show BP102 labeling. (B) wt embryo. (B' and B'') *CYFIP*^{85.1} embryos. Connectives and commissures are thicker than in wt (asterisks) and are not properly separated (arrowheads). (B'') Break in the longitudinal connectives (arrow). Panels (C)–(C'') show Fas II labeling of motor neurons. Two abdominal segments are shown. (C) wt embryo. (C' and C'') *CYFIP*^{85.1} embryos showing intersegmental nerve defects: axon stalling (arrow) and abnormal branching (asterisks). All images show stage 17 embryos. (A) and (B) panels: ventral views, anterior to the top; (C) panels: lateral views, anterior to the left. Scale bar, 20 μ m.

ing with monoclonal antibody BP102 (Figure 3B) revealed thickening of connectives and commissures (11% of mutant embryos, $n = 100$) (Figures 3B' and 3B'', asterisks) and occasional connective breaks (Figure 3B'', arrow). Finally, 10% of the mutant embryos show defects in motor axons that could be classified as stalling (Figure 3C', arrow) and abnormal branching, respectively (Figures 3C' and 3C'', asterisks) ($n = 100$).

Similar CNS and PNS defects were found in transheterozygous embryos carrying large IIIIR to Y chromosome transpositions (segment 88–93) and the *CYFIP* null mutation (data not shown). Furthermore, to provide final evidence that the observed phenotypes are specifically due to loss of *CYFIP*, we generated *UAS-CYFIP* transgenic animals. A third chromosome *UAS-CYFIP* transgene was recombined into the *CYFIP*^{85.1} null background (*UAS-CYFIP*, *CYFIP*). *CYFIP* mutant animals carrying the panneuronal *elav-Gal4* driver and the *UAS-CYFIP* transgene showed rescue of the midline crossing phenotype (79% crossing frequency in null embryos, 10% in rescued embryos; $n = 100$). Moreover, early pupal lethality was completely rescued, and some animals reached adulthood (2%; number of expected adults, $n = 400$).

Finally, using two driver copies further improved rescue, with viability reaching 76% ($n = 150$). In summary, *CYFIP* plays a role in guidance and morphology of central and peripheral axons.

CYFIP Regulates Synaptic Morphology at the NMJ

In humans, mice, and flies, lack of FMRP/dFMR1 results in synaptic changes (Hinton et al., 1991; Comery et al., 1997; Zhang et al., 2001). In *Drosophila*, the dFMR1 requirement for synapse development has been demonstrated at the larval NMJ. *dFMR1* deficiency results in synapse overgrowth, while dFMR1 overexpression leads to synapse undergrowth (Zhang et al., 2001). Because of these findings and since *CYFIP* localizes to embryonic NMJ at the time synaptogenesis takes place, we examined the structure of synaptic terminals in *CYFIP* mutants. Third instar larva muscle 4 type 1b terminal, one of simplest and most characterized terminals, has been considered for this analysis.

NMJ appears contracted in *CYFIP* mutants compared to wt (Figure 4A, panels 4Ac and 4Ad versus panels 4Aa and 4Ab). In the literature, the number of synaptic boutons has usually been used to characterize the size of synaptic terminals. In the case of *CYFIP*, this parameter cannot be used; synaptic boutons appear fused or not well developed, which makes it difficult to identify and measure their size and number (Figure 4A, panels 4Ac and 4Ad and magnification in 4Ad'). To statistically evaluate the *CYFIP* phenotype, we defined a new parameter: the total length of the synaptic terminal. In brief, NMJs were fluorescently labeled with synaptic marker anti-DLG and analyzed by conventional microscopy. Pictures were imported into an in-house developed software (NSURFX), which allowed us to automatically measure the length of the redrawn DLG-positive structure.

In *CYFIP* larvae, synaptic length is reduced to 67%–70% compared to that found in wt or revertant (precise excision) animals (71 versus 105 or 101 μ m, $p < 0.001$), a phenotype that is completely rescued by *elav-Gal4*-driven *CYFIP* expression (Figures 4B and 4C). A tendency for reduced synaptic length is already observed in heterozygous *CYFIP* animals ($p < 0.05$ versus wt, $p < 0.1$ versus revertants), a finding that suggests a dose-dependent effect. We also measured the synaptic length of *dFMR1* null NMJs (Figure 4A, panels 4Ae and 4Af), which show overgrowth, based on the number of boutons (Zhang et al., 2001). *dFMR1* larvae show a 20% length increase over wt controls (126 versus 105 μ m, $p < 0.001$) (Figure 4B), indicating that the two approaches (counting bouton number and measuring synaptic length) produce similar results. Loss of *CYFIP*, therefore, has an opposite effect to loss of dFMR1 on synapse growth.

A second striking feature of *CYFIP* NMJs is the occurrence of supernumerary buds (Figure 4A, panels 4Ac, 4Ad, and magnifications in 4Ac inset and 4Ad'). Buds arising from preexisting boutons have been described as an intermediate structure toward establishment of a new bouton (Zito et al., 1999). Synaptic terminals in *CYFIP* mutants exhibit about four to five times more buds than wt or revertant terminals (7.8 versus 1.6 or 2.0, $p < 0.001$) (Figure 4C). Thus, the *CYFIP* NMJ presents an overall immature aspect, likely due to a block in synapse differentiation.

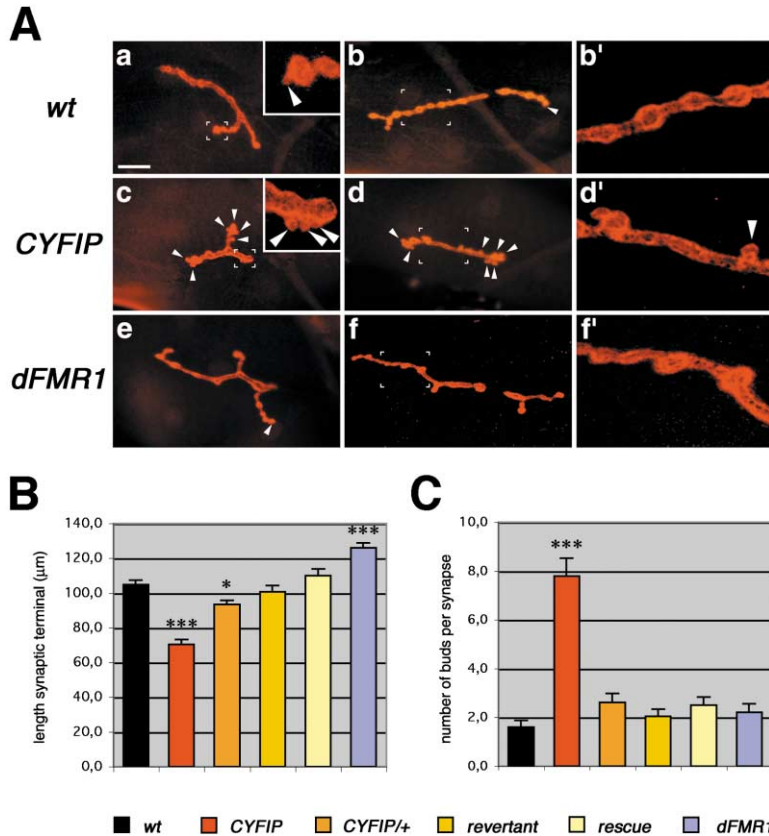


Figure 4. CYFIP Controls Synaptogenesis at NMJ

(A) DLG immunolabeling of muscle 4 synaptic terminals. Third instar larvae of the following genotypes: (Aa, Ab, and Ab') wt, (Ac, Ad, and Ad') *CYFIP*^{85.1}, and (Ae, Af, and Af') *dFMR1*. Compared to wt, *CYFIP* synapses display undergrowth, disturbed bouton structure, and supernumerary budding. *dFMR1* synapses display overgrowth. Insets in (Aa) and (Ac) show high magnification of marked regions. Arrowheads indicate buds. Panels (Ab'), (Ad'), and (Af') are high magnifications of marked regions in (Ab), (Ad), and (Af), respectively. Scale bar, 20 µm (Aa–Af), 3 µm (Ab', Ad', and Af').

(B and C) Statistic evaluation of NMJ phenotypes of the following genotypes: wt, *CYFIP*^{85.1} (*CYFIP*), *CYFIP*^{85.1} heterozygous (*CYFIP*/+), precise excision *CYFIP*^{70.1} (revertant), *elav-Gal4; UAS-CYFIP*, *CYFIP*^{85.1} (rescue), and *dFMR1*. Sample size (number of muscle 4 junctions scored) was 28 per genotype. Error bars indicate SEM; statistical significance was calculated using ANOVA and the Newman-Keuls method for post hoc pair-wise analyses. Significant differences versus wt are indicated on top of bars (*p < 0.05; ***p < 0.001).

(B) Length of synaptic terminals in microns, as measured using NSURFX software (see Experimental Procedures).

(C) Number of buds per synapse.

CYFIP Maternal Contribution

Several observations call for a CYFIP maternal contribution. First, axon tracts from null embryos are still faintly labeled with the CYFIP antibody (Figure 5A). Second, *CYFIP* RNA is highly expressed in ovaries (Figure 1A). Third, *CYFIP* RNA/protein are present very early during embryogenesis (Figures 1B and 1D). To determine whether CYFIP immunoreactivity in null embryos is of maternal origin, we compared the content of CYFIP in protein extracts from wt and *CYFIP* mutants [*EP(3)3267* and *CYFIP*^{85.1} homozygous] at embryonic and larval stages. Western blot analysis demonstrated that *EP(3)3267* is a hypomorphic allele that displays reduced CYFIP levels throughout development (Figure 5B). *CYFIP*^{85.1}, on the other hand, shows faint levels of expression in embryos but not in wandering larvae, in agreement with the observation that maternal contribution is generally no longer detectable at that stage. Based on the amount of protein present in null embryos, the amount of maternal contribution corresponds to 10%–15% of CYFIP expression in wt embryos (Figure 5B).

To determine the importance of the maternal contribution, we used the FLP/*ovo*^D system (Chou and Perrimon, 1996) and generated homozygous *CYFIP* mutant clones within the germline of heterozygous females. Deletion of both maternal and zygotic CYFIP leads to variable but dramatically enhanced nervous system defects (Figure 5C, compare with Figures 3A and 3A') and to embryonic lethality. These data indicate that the maternal contribution of CYFIP rescues nervous system defects and embryonic lethality.

Biochemical Interactions of CYFIP with dFMR1 and dRac1

Human CYFIP1 and CYFIP2 interact with FMRP (Schenck et al., 2001). Independently, CYFIP1 has been reported as a target for the Rac1 small GTPase (Kobayashi et al., 1998). In order to define the molecular role of *Drosophila* CYFIP, we asked whether the molecular interactions with FMRP and Rac1 fly orthologs are conserved. To test for dFMR1–CYFIP interaction in vitro, we used a GST–dFMR1 fusion (Schenck et al., 2002). GST–dFMR1 or GST alone was used in GST pull-down assays and incubated with in vitro-translated, radiolabeled luciferase as negative control, or with CYFIP. For this purpose, two largely overlapping CYFIP fragments were used (Figure 6A, top). Both of them interact with GST–dFMR1 but not with GST alone (Figure 6A). Luciferase was neither bound by GST nor by GST–dFMR1. Next, to confirm CYFIP–dFMR1 interaction, we immunoprecipitated endogenous CYFIP from cytoplasmic extracts of S2 cells transiently overexpressing dFMR1. dFMR1 coimmunoprecipitated with endogenous CYFIP. In contrast, no dFMR1 was found when an aliquot of the same extract was incubated with comparable amounts of rabbit IgG (Figure 6B).

We also performed coimmunoprecipitation experiments to check for dRac1–CYFIP interaction (Figure 6C). We transfected S2 cells with flag-tagged dRac1 constructs carrying either the constitutively active mutation V12 (dRac1V12) or the dominant-negative mutation N17 (dRac1N17) and precipitated the proteins via their flag tags. Endogenous CYFIP was found to coimmunopreci-

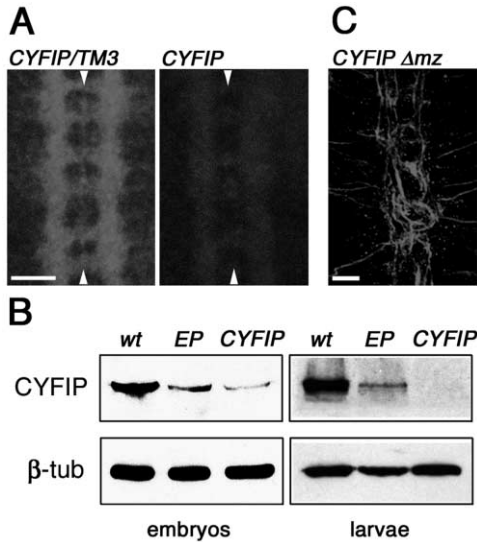


Figure 5. CYFIP Maternal Component

(A) CYFIP labeling in the ventral nerve cord of homozygous *CYFIP^{65.1}* embryos and heterozygous sibs at stage 17. Ventral views, anterior to the top. Arrowheads indicate midline, where CYFIP is also expressed. Residual immunolabeling is observed in zygotic null embryos.

(B) Western blot analysis in wild-type (wt), homozygous *EP(3)3267 (EP)*, homozygous *CYFIP^{65.1}* embryos (*CYFIP*) (stage 12–17), and in wandering L3 larvae of the same genotypes. The same blots were probed with anti- β -tubulin to show equivalent protein loading.

(C) Fas II labeling of an embryo devoid of maternal and zygotic CYFIP components (*CYFIP Δ mz*), revealing strongly disturbed CNS development (compare with wt and *CYFIP* zygotic mutant embryos, Figure 3, panels 3A–3A').

(A–C) Scale bars, 20 μ m.

pitiate with dRac1V12 but not with dRac1N17. No CYFIP was found in a control anti-flag precipitation using an equal amount of nontransfected extract. Therefore, CYFIP interacts with dRac1 in an activity-dependent manner. In the same experiment, endogenous dFMR1 was not found to coimmunoprecipitate with dRac1V12 and CYFIP (data not shown). CYFIP may thus be present in two alternative complexes, associated with either dFMR1 or with dRac1. Small GTPases are thought to act by modifying the conformation of their effector proteins, which are normally bound by the GTPases in their active state (Bishop and Hall, 2000). The activity-dependent interaction with dRac1 suggests that CYFIP represents such a Rac1 effector protein.

CYFIP Antagonizes dRac1 and dFMR1 in the Eye

To gain insights into the signaling cascade involving dRac1, CYFIP, and dFMR1, we performed genetic interaction experiments. Since unbalance between gene products that work in the same pathway often induces a mutant phenotype, we overexpressed the three genes in the eye using the *GMR-Gal4* driver. No effect on eye morphology upon CYFIP overexpression could be detected (Figure 7B). Overexpression of dRac1V12, on the other hand, caused a mild rough phenotype, indicative of ommatidia misorganization, and complete loss of ommatidia in the posterior region (Figure 7D, asterisk).

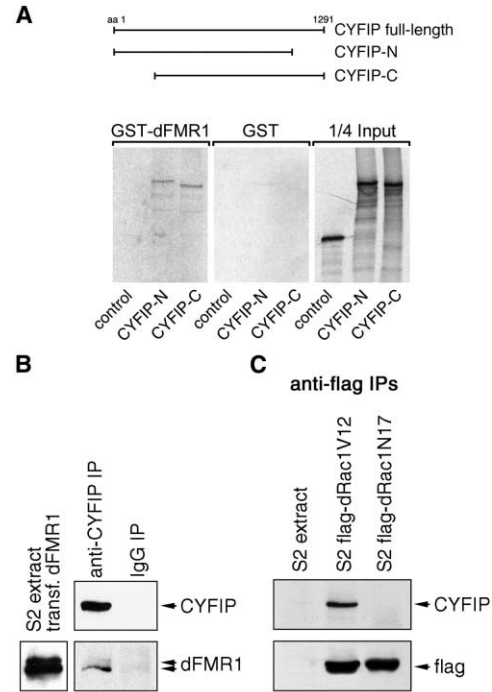


Figure 6. CYFIP Interacts In Vitro and In Vivo with dFMR1 and dRac1

(A) Pull-down assay between GST-tagged dFMR1 and in vitro-translated CYFIP fragments or between GST-dFMR1 and Luciferase (control) in the presence of 150 mM NaCl. CYFIP-N and CYFIP-C indicate two overlapping fragments carrying the N- (aa 1–1152) and the C-terminal part (aa 167–1291) of CYFIP, respectively. In the Input lanes, 25% of the translation products used in a reaction were loaded. CYFIP but not luciferase interacts with dFMR1. None of them unspecifically interact with GST alone.

(B) Western blot showing interaction between endogenous CYFIP and transiently overexpressed dFMR1 in S2 cells. Material loaded is indicated on top of each lane (anti-CYFIP IP, extract + anti-CYFIP; IgG IP, extract + rabbit IgG), proteins revealed by Western blot to the right of each panel. Anti-CYFIP but not IgG coimmunoprecipitates dFMR1 (comparable amounts of antibodies were used). Anti-dFMR1 reveals two bands at 85 and 92 kD, as described in Schenck et al. (2002).

(C) Anti-flag coimmunoprecipitation experiments revealing activity-dependent interaction between overexpressed dRac1 and endogenous CYFIP. As in (B), loaded material is indicated on top of each lane, proteins revealed by Western blot to the right of each panel. CYFIP specifically coimmunoprecipitates with flag-dRac1V12 (lane in the middle) but not with flag-dRac1N17 (lane to the left).

Cooverexpression of dRac1V12 and CYFIP partially rescued the two phenotypes (Figure 7E, asterisk), while cooverexpression of an unrelated protein, β -gal, had no effect on the dRac1V12 phenotype. The observed antagonistic interaction between dRac1 and CYFIP was subsequently confirmed by using a sensitized background. dRac1V12 overexpression in flies that carry only half a dose of CYFIP show a much stronger phenotype compared to that observed in wt flies overexpressing dRac1V12 (Figure 7F, asterisk). Eyes are strongly reduced in size and flattened. The entire posterior half of these eyes has lost ommatidia and is deformed; ommatidia in the rest of the eye are not distinct from each other. In summary, CYFIP overexpression suppresses the rough eye phenotype due to overexpression of con-

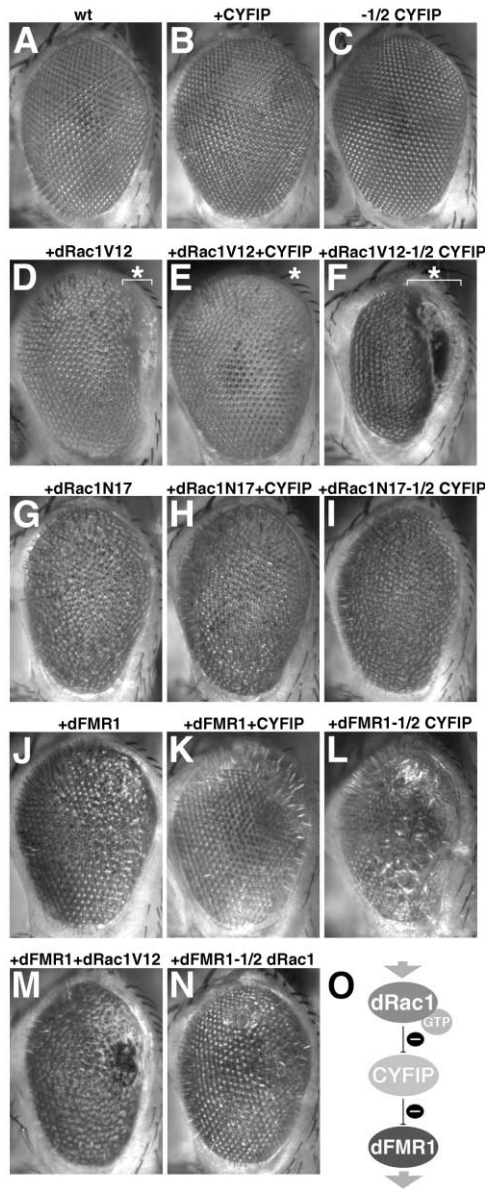


Figure 7. dRac1, CYFIP, and dFMR1 Dosage-Dependent Interactions In Vivo

On top of each eye, overexpressed proteins are indicated by "+", reduced protein levels by "-". (A) Wild-type (wt). (B, D-O) *GMR-Gal4* driven expression. (B) *UAS-CYFIP/TM3*, (C) *CYFIP*+, (D) *UAS-Rac1V12/TM3*, (E) *UAS-Rac1V12/UAS-CYFIP*, (F) *UAS-Rac1V12/CYFIP*, (G) *UAS-Rac1N17/+*, (H) *UAS-Rac1N17/UAS-CYFIP*, (I) *UAS-Rac1N17/CYFIP*, (J) *UAS-dFMR1/TM3*, (K) *UAS-dFMR1/UAS-CYFIP*, (L) *UAS-dFMR1/CYFIP*, (M) *UAS-dFMR1/UAS-Rac1V12*, (N) *UAS-dFMR1/Df(3L)Ar14-8*. Asterisk in panel (D) marks the posterior region of the dRac1V12 overexpressing eye, which has lost ommatidia structure. Asterisks in panels (E) and (F) mark the corresponding region in eyes with elevated or reduced levels of CYFIP. *UAS-CYFIP* and *UAS-dFMR1* indicate EP-lines *EP(3)3267* and *EP(3)3517*, respectively. For all genotypes, male eyes of representative phenotype are shown. All flies were maintained at 25°C. (O) Model for dRac1, CYFIP, and dFMR1 signaling pathway.

stitutively active Rac1, while loss of one dose of *CYFIP* enhances that phenotype.

The same *CYFIP* allelic combinations were used with

flies carrying *UAS-dRac1N17*, the dominant-negative form of dRac1. As reported by Chang and Ready (2000), eye overexpression of dRac1N17 also induces a rough eye phenotype. Indeed, constitutively active and dominant-negative small GTPase mutants often produce similar rather than opposite phenotypes, as expected from molecules that have a cyclic mode of action (Luo, 2000). In contrast to the strong interactions observed with the activated form of dRac1, we did not detect an influence of CYFIP dosage in this analysis (Figures 7G–7I). The finding that overexpression of CYFIP cannot rescue the dRac1N17 overexpression phenotype is likely due to the inability of dRac1N17 to bind (see above) and activate its effector CYFIP.

Overexpression of dFMR1 affects eye morphology (*sevenless-Gal4*; Wan et al., 2000; Zhang et al., 2001) (*GMR-Gal4*; Figure 7J). Overexpression of CYFIP partially rescues ommatidia misorganization caused by dFMR1 overexpression (Figure 7K). In contrast, dFMR1 overexpression in heterozygous *CYFIP* flies results in an enhanced phenotype: eyes are of reduced size and contain areas lacking distinct ommatidia (Figure 7L). This led us to conclude that, like CYFIP and dRac1, CYFIP and dFMR1 stand in an antagonistic relationship, in perfect agreement with the opposite effects of dFMR1 and CYFIP loss on synapse morphology.

To further characterize the relationship among the three players, we also asked whether *dRac1* and *dFMR1* genetically interact. For this purpose, we overexpressed dFMR1 in genetic backgrounds of either elevated or reduced dRac1 levels. The latter was achieved by using a deficiency, *Df(3L)Ar14-8*, that uncovers *dRac1* (Hu et al., 2001). Cooverexpressing dFMR1 and dRac1 has a more severe phenotype than overexpressing either of the two proteins (Figure 7M versus 7D and 7J). Eyes overexpressing dRac1 and dFMR1 appear narrowed and show large ommatidia that are reduced in number compared to wt. We also observed areas containing degenerating ommatidia. On the other hand, overexpressing dFMR1 in eyes that have half a dose of *dRac1* partially rescues the mutant phenotypes observed in eyes that are wild-type for *dRac1* and that overexpress dFMR1 (Figure 7N versus 7J).

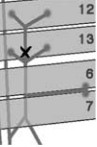
In summary, the eye phenotype of flies overexpressing dFMR1 is enhanced by dRac1 overexpression and suppressed by reduced dRac1 expression.

CYFIP Antagonizes dRac1 and dFMR1 in the Nervous System

To test whether the antagonistic dRac1-CYFIP and CYFIP-dFMR1 interactions reflect the general mode of action of these molecules, we performed gene dosage experiments in the nervous system and confirmed our finding of CYFIP antagonizing dRac1 and dFMR1 (Table 1). In this case, *elav-Gal4* was used as a driver.

To investigate the effect of CYFIP dosage on neuronal dRac1V12 overexpression, we scored for the premature arrest phenotype of intersegmental motor nerve b (ISNb), which has been previously reported for dRac1V12 (Kaufmann et al., 1998). In *elav-dRac1V12* embryos, 29% of ISNb were arrested at the site of contact with ventral longitudinal muscle 13 before reaching their final target, muscle 12 (see Table 1, schematic illustration) (27%

Table 1. Genetic Interactions in the Nervous System

A. dRac1V12-CYFIP in Axonogenesis				
	+dRac1V12	+dRac1V12+CYFIP	+dRac1V12 -1/2CYFIP	
Aberrant midline crossing	0% (n = 135)	0% (n = 90)	8% (n = 105)	
ISNb premature arrest				
	normal growth	71%	83%	40%
	partial arrest	27%	16%	53%
	complete arrest	2% (n = 348)	1% (n = 244)	7% (n = 307)
B. CYFIP-dFMR1 at the NMJ				
	+dFMR1	+dFMR1 +CYFIP	+dFMR1 -1/2CYFIP	
Synaptic terminal length (wt = 105 ± 3 μm)	70 ± 4 μm (n = 28)	89 ± 5 μm (n = 28)	65 ± 3 μm (n = 28)	

Aberrant midline crossing: n = number of embryos scored. % indicates percentage of embryos showing at least one ectopic midline crossing of FasII-labeled fascicles.

ISNb premature arrest: n = number of embryonic stage 17 abdominal hemisegments A2-A7 scored. Wt ISNb nerves extend to contact distal muscle 12 (see schematic drawing). Complete arrest indicates ISNb nerves that completely stop at the site of contact with muscle 13 (X). Partial arrest indicates cases in which at least 50% of ISNb motor fibers stop at the site of contact with muscle 13. See Supplemental Data online.

Synaptic terminal length has been determined as in Figure 4 and is indicated ± SD. n = number of muscle 4 synapses scored. Genotypes are according to Figure 7, using *elav-Gal4* as a driver.

partial + 2% complete arrest). Cooverexpressing CYFIP reduced the frequency of the dRac1V12 arrest phenotype to 17% (16% + 1%; $p < 0.05$; X^2 versus +dRac1V12). Accordingly, reducing CYFIP dosage strongly increased it: partial ISNb stalling reaches 53%, complete stalling, 7% ($p < 0.001$; X^2 versus +dRac1V12).

Additional striking evidence for genetic interaction between dRac1V12 and CYFIP in the nervous system came from the analysis of central axons. Neither embryos overexpressing dRac1V12 nor heterozygous CYFIP null embryos ever showed ectopic midline crossing, whereas 8% of embryos overexpressing dRac1V12 in heterozygous *CYFIP* background showed these axon guidance errors (Table 1A). Thus, as in the eye, CYFIP antagonizes activated dRac1 in motor axon outgrowth and in pathfinding at the midline choice point.

One of the most striking dFMR1 phenotypes observed during nervous system differentiation concerns the neuromuscular junction (Zhang et al., 2001). Neuronal dFMR1 overexpression causes synaptic undergrowth, as visualized by the reduced average synaptic length: 105 μm in wt (see above) and 70 μm upon dFMR1 overexpression (+dFMR1; $p < 0.001$ versus wt; ANOVA) (Table 1). While cooverexpression of a control (β -gal) had no effect on the dFMR1 overexpression phenotype (data not shown), cooverexpression of CYFIP rescued synapse length to an average of 89 μm (+dFMR1 + CYFIP; $p < 0.001$ versus +dFMR1; ANOVA). Finally, decreasing CYFIP dosage in the dFMR1 overexpressing synapses showed the tendency to further reduce synaptic length (+dFMR1-1/2CYFIP; $p < 0.5$ versus +dFMR1; ANOVA), altogether suggesting that the antagonistic relation between CYFIP and dFMR1 is also conserved in the nervous system.

Discussion

Neuronal morphogenesis and connectivity require actin cytoskeleton remodeling as well as local translation in response to extracellular signals (reviewed in Luo, 2002; Steward and Schuman, 2001). Synaptic plasticity, a mechanism of information storage in learning and memory, also involves these processes (Martin et al., 2000). Here we present data indicating that the CYFIP adaptor molecule directly interacts with two classes of proteins that are involved in such processes. Understanding the molecular link between cytoskeleton reorganization and local control of translation is an important topic, as it will help us to elucidate the molecular bases of neuronal plasticity and learning.

CYFIP: The Missing Link

Mutations in Rho GTPases, which control cytoskeleton reorganization, affect wiring in neuronal cell systems and animal models (reviewed in Luo, 2002). Moreover, defects in their pathways are associated with mental retardation in humans (reviewed in Ramakers, 2002; Chelly and Mandel, 2001; Luo, 2000) and with altered dendritic spines in animal models (Meng et al., 2002; Luo et al., 1996) and cultured rat hippocampal slices (Nakayama et al., 2000).

A growing body of evidence indicates that local protein synthesis is a key feature of synaptic plasticity (reviewed in Steward and Schuman, 2001). All the machinery necessary for protein synthesis is present at the site of synaptic contact (Steward and Levy, 1982). In addition, local protein synthesis occurs in live transected dendrites (Torre and Steward, 1992). It has been recently proposed that FMRP, the protein absent in frag-

ile X mental retardation syndrome, and its *Drosophila* ortholog regulate translation (Laggerbauer et al., 2001; Li et al., 2001; Brown et al., 2001; Zhang et al., 2001), in particular at the synapse (Greenough et al., 2001; Zalfa et al., 2003; Miyashiro et al., 2003). FMRP is indeed associated with polyribosomes (Corbin et al., 1997; Feng et al., 1997), its synthesis being increased in response to neurotransmitter activation in distal dendrites (Weiler et al., 1997). All these results call for a role of FMRP in the control of local protein synthesis underlying synaptic plasticity (Greenough et al., 2001).

Loss of FMRP in human patients and in the fragile X mouse model causes synaptic abnormalities (changed number and shape of dendritic spines) (Comery et al., 1997; Irwin et al., 2000) strikingly resembling those observed in mutants affecting Rac1 signaling pathways. The convergent phenotypes of mutations affecting FMRP and Rho GTPase pathways suggest a molecular link in neuronal remodeling. Moreover, FMRP interacting protein CYFIP1 (Schenck et al., 2001) has been shown to interact with Rac1 (Kobayashi et al., 1998). Here we provide biochemical and genetic evidence that CYFIP, the fly ortholog, interacts with dRac1 and dFMR1, thus establishing in vivo that these molecules act in a common pathway. Lack of motifs typical of proteins that regulate Rho GTPase activity, such as GTPase activating proteins (GAPs) (Scheffzek et al., 1998) and guanine nucleotide exchange factors (GEFs) (Schmidt and Hall, 2002), makes it unlikely that CYFIP acts upstream of dRac1. In addition, the activity-dependent interaction suggests that CYFIP acts as a dRac1 effector. Indeed, Rho GTPases only bind and transduce their signals to downstream targets once in the activated GTP-bound state.

It is very likely that in vertebrates, too, FMRP and the Rac1 pathway, both implicated in cognitive functions, are connected through CYFIP proteins. Indeed, mouse/human CYFIP1 (Koster et al., 1998; Schenck et al., 2001), FMRP (Agulhon et al., 1999; Weiler et al., 1997), and Rac1 (Hall, 1994; Nakayama et al., 2000) are widely expressed in the developing as well as in the adult nervous system and are present at synapses. All three proteins share strong expression in the hippocampus, known for its role in learning and memory. CYFIP2 is also present at synapses (Schenck et al., 2001). Understanding the role of CYFIP1 and CYFIP2 in mammals awaits the characterization of single and/or double mouse knockout phenotypes or the identification of mental retardation syndromes associated with CYFIP1/2 mutations.

CYFIP Controls Synaptogenesis and Axonogenesis

Consistent with the CYFIP expression profile, mutants show defects at the neuromuscular junction. *Drosophila* NMJs share a number of features with central excitatory synapses in the vertebrate brain and constitute the synaptic plasticity model in *Drosophila* (reviewed in Koh et al., 2000). In vivo studies on fly NMJ have shown that new synaptic boutons are added by the budding of pre-existing ones (Zito et al., 1999). In *CYFIP* mutants, synapse terminals are shorter and display a higher number of buds than in wt animals, indicative of impaired syn-

apse growth. Loss of *dFMR1* (Zhang et al., 2001) therefore produces a NMJ phenotype that is opposite to that of *CYFIP* null flies. Our in vivo data support the idea that Rac1 is involved in the formation of synaptic motor terminals. In the future, the analyses of loss of function mutations will clarify the role of Rho GTPases at the synapse.

In addition to the synapse, *CYFIP* mutations affect other aspects of neuronal morphogenesis: axonal pathfinding (midline crossing), growth (motor axon stalling), and branching (ectopic motor axon branching). Defects in these processes are also shared by *dRac1* and *dFMR1* mutants (Kaufmann et al., 1998; Ng et al., 2002; Hakeda-Suzuki et al., 2002; Morales et al., 2002; Dockendorff et al., 2002), which further supports the idea that *Drosophila* Rac1, CYFIP, and dFMR1 work in the same pathway. Gene dosage experiments in the eye and in the nervous system suggest a negative regulation between dRac1 and CYFIP as well as between CYFIP and dFMR1, which results in an agonistic relationship between dRac1 and dFMR1. Based on biochemical and genetic data, we therefore propose a model (Figure 7O) in which dRac1 activation upon unknown extracellular signals positively regulates dFMR1 action on neuronal morphogenesis.

Interestingly, the frequency of axonal defects observed in *CYFIP* embryos seems lower compared to that found in *Drosophila* Rac mutants (Hakeda-Suzuki et al., 2002). Moreover, axons abnormally crossing the midline were observed in *CYFIP* and Rac mutants (Hakeda-Suzuki et al., 2002) but not in *dFMR1* mutants (data not shown). There are several non-mutually exclusive explanations for such differences. First, distinct extracellular cues activate a Rho GTPase differentially in time and space, which may engage several downstream effector pathways. Lack of CYFIP may affect some of the pathways activated by dRac1. Similarly, mutations in the Rho GTPase GEF Trio and in its regulator, the receptor tyrosine phosphatase Dlar, do not show identical axonal phenotypes (Newsome et al., 2000; Bateman et al., 2000; Krueger et al., 1996). The cell-specific requirement of gene interaction may also reflect differences in the profile of expression; while CYFIP accumulates in specific axonal tracts and at synapses, dFMR1 seems to be more widely distributed (Wan et al., 2000; Zhang et al., 2001). Second, part of the null phenotypes may be hidden by the presence of RNA and/or protein loaded into the egg, as shown in the case of *CYFIP*. Indeed, *dFMR1* has been reported to be expressed maternally (Wan et al., 2000; Schenck et al., 2002). The maternal requirement of *dRac1* and *dFMR1* remains to be assessed.

Together with the data obtained in *dFMR1* flies, our results raise the question as to whether axons also show abnormalities in fragile X syndrome. So far, this has not been reported in patients nor in the mouse FMRP knockout model; however, an implication of this protein in axonogenesis could be hidden by the presence of FMRP-related FXR1 and FXR2 proteins. Indeed, FXR2P is expressed in a pattern very similar to that of FMRP (Bakker et al., 2000; Agulhon et al., 1999), and some behavioral phenotypes in the *FXR2* knockout mice resemble those observed in *FMR1* null mice (Bontekoe et al., 2002). Moreover, detection of subtle defects may require a detailed analysis. Defects might be specific

to axonal subsets, as has been shown in *dFMR1* flies (Morales et al., 2002; Dockendorff et al., 2002).

The promiscuity of neuronal defects observed in the CYFIP mutants suggests a general role of the protein in actin cytoskeleton reorganization via Rho GTPase pathways. Such a role is in agreement with the association of CYFIP molecules with Rac1 (Kobayashi et al. [1998] and the present study) and with CYFIP1 cosedimenting with actin in vitro (Kobayashi et al., 1998). It is generally thought that Rac activation promotes neurite extension, and it has been recently shown that WAVE1-induced actin nucleation depends on Rac1 (Eden et al., 2002). The WAVE1 protein forms an inactive complex also containing the CYFIP2 protein (also called PIR121), which dissociates upon interaction with activated Rac1 (Eden et al., 2002). The dissociation into subcomplexes releases activated WAVE1, which in turn stimulates actin nucleation (Eden et al., 2002). We speculate that, simultaneously, CYFIP may be released to regulate dFMR1/FMRP-mediated translational control. Hence, CYFIP may be a protein factor at the crossroads between control of actin cytoskeleton and control of local protein translation in neurons. In the future, it will be important to dissect the dRac1 pathways in which CYFIP and dFMR1 are involved and to understand the implication of these pathways in the cognitive defects of fragile X syndrome.

Experimental Procedures

Genetics

The wild-type strain was *Sevelen*. Transposon insertion lines *EP(3)3267* and *EP(3)3517* (Rorth, 1996) were provided by the Szeged Stock Center. *GMR-Gal4* (*ninaE.GMR-Gal4*), *elav-Gal4* (C155), *Df(3L)Ar14-8*, *Df(3R)ea*, *Tp(3;Y)B150*, and *Tp(3;Y)L58* were obtained from the Berkeley Stock Center. *UAS-dRac1V12* and *UAS-dRac1N17* flies (Luo et al., 1994) were provided by D. Ready, and *dFMR1* null strain $\Delta 113M$ (Zhang et al., 2001; Morales et al., 2002) by B. Hassan. *CYFIP* mutants were obtained upon P element mobilization in *EP(3)3267* after isogenization. Excision lines were characterized by PCR. Transgenic lines were obtained using standard protocols. *FRT82B* and *UAS-CYFIP* (line 12.2) were recombined onto the *CYFIP*^{85.1} chromosome. Germline clones were induced in *hs-FLP; FRT82B ovo^D/FRT82B CYFIP*^{85.1} flies as described (Chou and Perrimon, 1996).

Molecular Techniques

Poly(A)⁺ RNA was recovered from wt flies/tissues of the indicated developmental stages, using the Quickprep mRNA purification kit (Pharmacia). The *CYFIP* probe (2.9 kb fragment amplified by PCR from EST-clone LD47929) and the 0.5 kb ribosomal protein 49 probe were P³²-labeled by random priming. DNA constructs: the *CYFIP* N terminus was amplified by PCR using primers GGGGAATTCAGCC CAGCATGACGGAGAAG and GGGAGAGCATATGCACGCAAATGT TGACCAC and *CYFIP* EST clone LD47929 as a template. The amplified fragment was cloned by EcoRI, NdeI digestion in front of the C-terminal part of the coding sequence (EST LD19991/pBluescript). *dRac1* was amplified by PCR from genomic DNA using primers GG GGTACCACCATGGACTACAAAGACGATGACGATAAACAGG CGATCAAGTGCCTGCTC (containing flag) and GGGGGTACCTTA GAGCAGGGCGCACTTGCG and cloned in the pPac vector as KpnI fragment. The V12 and N17 mutations were introduced by site-directed mutagenesis using TCGTGGGCGACGTAGCCGTGGGA AAG (V12), GCCGTGGGAAAGAAGTGCCTGCTGATC (N17), and complementary primers, respectively.

Cell Culture, Transient Transfection, and Total Protein Extracts

S2 cells were cultured in Schneider cell medium (Gibco BRL) plus 10% fetal calf serum and transfected using Effectene reagent (Qia-

gen). For Western blot on S2 extract, the cell pellet was lysed in 1 × SDS-PAGE loading buffer and subjected to SDS-PAGE analysis. For embryonic and larval extracts, nonfixed animals (without or after X-gal staining) were mashed with a pestle in 150 mM NaCl, 20 mM Tris-HCl (pH 7.5), 1 mM EDTA, 0.1 mM MgCl₂, 1% Triton X-100, and protease inhibitor cocktail (PIC). The supernatant of a 12,000 × g centrifugation was briefly sonicated, and the amount of total protein was determined by Bradford assay.

In Situ Hybridization, Immunolabeling, and Western Blot Analysis

In situ hybridization using digoxigenin-labeled riboprobes and immunolabeling was performed according to standard procedures. *CYFIP*-specific riboprobes were generated from EST clone LD47929. For CG6226-specific in situ hybridization, a riboprobe was generated from EST-clone LD33762. A peptide in the central region of CYFIP was used for rabbit immunization and affinity purification of polyclonal anti-CYFIP antibody #1719 (used at 1:100). Other primary antibodies were anti-Fas II (1:50) (gift of C. Goodman), anti-DLG (1:400) (gift of P. Bryant), BP102 (1:100), 22C10 (1:20) (DSHB), anti-β-gal (1:500) (Sigma, Cappel), and anti-β-tubulin (Chemicon) (1:4000). Secondary antibodies (Jackson) coupled with Cy3 or FITC were used at 1:400, HRP conjugated antibodies at 1:10,000. For evaluation of NMJs, larvae open-book preparations were performed as described in Bellen and Budnik (2000). Pictures of all synapses were imported in the in-house developed NSURFX software that quantified the synaptic length by automatic measurement of the redrawn synaptic terminals.

Biochemical Interaction Assays

For immunoprecipitations, cytoplasmic extracts were prepared by lysing S2 cells in buffer (300 mM NaCl, 20 mM Tris-HCl [pH 7.5], 5 mM MgCl₂, 0.4% Triton X-100, PIC). The supernatant of a 2000 × g centrifugation was incubated with appropriate antibodies and protein A Sepharose. Anti-flag-dRac1 V12 and N17 immunoprecipitations were performed using extracts expressing the two mutant proteins at a similar level and using beads covalently linked to anti-flag antibody M2 (Sigma). Beads were washed extensively in lysis buffer, boiled in SDS-PAGE loading buffer, and subjected to SDS-PAGE analysis. The GST-dFMR1 pull-down assay has been previously described (Schenck et al., 2002).

Microscopy

The confocal microscope was a Leica TCS4D. Fluorescence images in one focal plane were obtained using a Zeiss Axiophot2 microscope. Images of *Drosophila* eyes were taken on a Leica Macro- scope M420 at seven focal planes and assembled using an in-house developed software.

Acknowledgments

We thank B. Hassan, P. Heitzler, D. Ready, the Szeged and Berkeley Stock Centers, P. Bryant, C. Goodman, and the Developmental Studies Hybridoma Bank for providing fly strains and antibodies. We are indebted to M. Kammerer for Northern blots, to C. Diebold and J. Sanny for technical assistance, and to all members of the Giangrande laboratory for comments on the manuscript. We thank D. Helminger, G. Duval, M. Boeglin, D. Hentsch, and J.L. Vonesch for help with statistics, antibody production, confocal microscopy, and development of software used in this study. Thanks to P. Heitzler for helpful discussions. This work was supported by funds from the Human Frontier Science Program (RGP0052/2001), National Institutes of Health (R01 HD40612-01), Institut National de la Santé et de la Recherche Médicale, the Centre National de la Recherche Scientifique, by FRAXA foundation, by Université Louis Pasteur, and by the Foundation pour la Recherche Médicale (FRM). A.S. was supported by the Ernst Schering Research Foundation and FRM, C.L. by a Natural Sciences and Engineering Research Council of Canada scholarship. N.H. was funded by grants from the National Cancer Institute of Canada and the Canadian Institutes of Health Research.

Received: December 5, 2002
Revised: April 15, 2003
Accepted: April 29, 2003
Published: June 18, 2003

References

- Agulhon, C., Blanchet, P., Kobetz, A., Marchant, D., Faucon, N., Sarda, P., Moraine, C., Sittler, A., Biancalana, V., Malafosse, A., and Abitbol, M. (1999). Expression of FMR1, FXR1 and FXR2 genes in human prenatal tissues. *J. Neuropathol. Exp. Neurol.* **58**, 867–880.
- Bakker, C.E., de Diego Otero, Y., Bontekoe, C., Raghoe, P., Luteijn, T., Hoogeveen, A.T., Oostra, B.A., and Willemsen, R. (2000). Immunocytochemical and biochemical characterization of FMRP, FXR1P, and FXR2P in the mouse. *Exp. Cell Res.* **258**, 162–170.
- Bardoni, B., and Mandel, J.L. (2002). Advances in understanding of fragile X pathogenesis and FMRP function, and in identification of X linked mental retardation genes. *Curr. Opin. Genet. Dev.* **12**, 284–293.
- Bardoni, B., Schenck, A., and Mandel, J.L. (1999). A novel RNA-binding nuclear protein that interacts with the fragile X mental retardation (FMR1) protein. *Hum. Mol. Genet.* **8**, 2557–2566.
- Bardoni, B., Schenck, A., and Mandel, J.L. (2001). The fragile X mental retardation protein. *Brain Res. Bull.* **56**, 375–382.
- Bateman, J., Shu, H., and Van Vactor, D. (2000). The guanine nucleotide exchange factor trio mediates axonal development in the *Drosophila* embryo. *Neuron* **26**, 93–106.
- Bellen, H.J., and Budnik, V. (2000). The neuromuscular junction. In *Drosophila Protocols*, W. Sullivan, M. Ashburner, and R.S. Hawley, eds. (New York: Cold Spring Harbor Laboratory Press), pp. 175–200.
- Bishop, A.L., and Hall, A. (2000). Rho GTPases and their effector proteins. *Biochem. J.* **348**, 241–255.
- Bontekoe, C.J.M., McIlwain, K.L., Nieuwenhuizen, I.M., Yuva-Paylor, L., Nellis, A., Willemsen, R., Fang, Z., Kirkpatrick, L., Bakker, C.E., McAninch, R., et al. (2002). Knockout mouse model for Fxr2: a model for mental retardation. *Hum. Mol. Genet.* **11**, 487–498.
- Brown, V., Jin, P., Ceman, S., Darnell, J.C., O'Donnell, W.T., Tenebaum, S.A., Jin, X., Wilkinson, K.D., Keene, J.D., and Darnell, R.B. (2001). Microarray identification of FMRP-associated brain mRNAs and altered mRNA translational profiles in fragile X syndrome. *Cell* **107**, 12–20.
- Campos-Ortega, J.A., and Hartenstein, V. (1985). *The Embryonic Development of Drosophila Melanogaster* (Berlin: Springer-Verlag).
- Caudy, A.A., Myers, M., Hannon, G.J., and Hammond, S.M. (2002). Fragile X-related protein and VIG associate with the RNA interference machinery. *Genes Dev.* **16**, 2491–2496.
- Chang, H.Y., and Ready, D.F. (2000). Rescue of photoreceptor degeneration in rhodopsin-null *Drosophila* mutants by activated Rac1. *Science* **290**, 1978–1980.
- Chelly, J., and Mandel, J.L. (2001). Monogenic causes of X-linked mental retardation. *Nat. Rev. Genet.* **2**, 669–679.
- Chou, T.B., and Perrimon, N. (1996). The autosomal FLP-DFS technique for generating germline mosaics in *Drosophila melanogaster*. *Genetics* **144**, 1673–1679.
- Comery, T.A., Harris, J.B., Willems, P.J., Oostra, B.A., Irwin, S.A., Weiler, I.J., and Greenough, W.T. (1997). Abnormal dendritic spines in fragile X knock-out mice: Maturation and pruning deficits. *Proc. Natl. Acad. Sci. USA* **94**, 5401–5404.
- Corbin, F., Bouillon, M., Fortin, A., Morin, S., Rousseau, F., and Khandjian, E.W. (1997). The fragile X mental retardation protein is associated with poly(A)⁺ mRNA in actively translating polyribosomes. *Hum. Mol. Genet.* **6**, 1465–1472.
- Darnell, J.C., Jensen, K.B., Jin, P., Brown, V., Warren, S.T., and Darnell, R.B. (2001). Fragile X mental retardation protein targets G quartet mRNAs important for neuronal function. *Cell* **107**, 1–11.
- Dockendorff, T.C., Su, H.S., McBride, S.M., Yang, Z., Choi, C.H., Siwicki, K.K., Sehgal, A., and Jongens, T.A. (2002). *Drosophila* lacking *dfmr1* activity show defects in circadian output and fail to maintain courtship interest. *Neuron* **34**, 973–984.
- Eden, S., Rohatgi, R., Podtelejnikov, A.V., Mann, M., and Kirschner, M.W. (2002). Mechanism of regulation of WAVE1-induced actin nucleation by Rac1 and Nck. *Nature* **418**, 790–793.
- Feng, Y., Absher, D., Eberhart, D.E., Brown, V., Malter, H.E., and Warren, S.T. (1997). FMRP associates with polyribosomes as an mRNP, and the I304N mutation of severe fragile X syndrome abolishes this association. *Mol. Cell* **1**, 109–118.
- Greenough, W.T., Klintsova, A.Y., Irwin, S.A., Galvez, R., Bates, K.E., and Weiler, I.J. (2001). Synaptic regulation of protein synthesis and the fragile X protein. *Proc. Natl. Acad. Sci. USA* **98**, 7101–7106.
- Hakeda-Suzuki, S., Ng, J., Tzu, J., Dietzl, G., Sun, Y., Harms, M., Nardine, T., Luo, L., and Dickson, B.J. (2002). Rac function and regulation during *Drosophila* development. *Nature* **416**, 438–442.
- Hall, A. (1994). Small GTP-binding proteins and the regulation of the actin cytoskeleton. *Annu. Rev. Cell Biol.* **10**, 31–54.
- Hall, A. (1998). Rho GTPase and actin cytoskeleton. *Science* **279**, 509–514.
- Hinton, V.J., Brown, W.T., Wisniewski, K., and Rudelli, R.D. (1991). Analysis of neocortex in three males with the fragile X syndrome. *Am. J. Med. Genet.* **41**, 289–294.
- Hu, H., Marton, T.F., and Goodman, C.S. (2001). Plexin B mediates axon guidance in *Drosophila* by simultaneously inhibiting active Rac and enhancing RhoA signaling. *Neuron* **32**, 39–51.
- Irwin, S.A., Galvez, R., and Greenough, W.T. (2000). Dendritic spine structural anomalies in fragile-X mental retardation syndrome. *Cereb. Cortex* **10**, 1038–1044.
- Ishizuka, A., Siomi, M.C., and Siomi, H. (2002). A *Drosophila* fragile X protein interacts with components of RNAi and ribosomal proteins. *Genes Dev.* **16**, 2497–2508.
- Kaufmann, N., Wills, Z.P., and Van Vactor, D. (1998). *Drosophila* Rac1 controls motor axon guidance. *Development* **125**, 453–461.
- Kobayashi, K., Kuroda, S., Fukata, M., Nakamura, T., Nagase, T., Nomura, N., Matsuura, Y., Yoshida-Kubomura, Y., Iwamatsu, A., and Kaibuchi, K. (1998). p140Sra-1 (Specifically Rac1-associated Protein) is a novel specific target for Rac1 small GTPase. *J. Biol. Chem.* **273**, 291–295.
- Koh, Y.H., Gramates, L.S., and Budnik, V. (2000). *Drosophila* larval neuromuscular junction: molecular components and mechanisms underlying synaptic plasticity. *Microsc. Res. Tech.* **49**, 14–25.
- Koster, F., Schinke, B., Niemann, S., and Hermans-Borgmeyer, I. (1998). Identification of shyc, a novel gene expressed in the murine developing and adult nervous system. *Neurosci. Lett.* **252**, 69–71.
- Krueger, N.X., Van Vactor, D., Wan, H.I., Gelbart, W.M., Goodman, C.S., and Saito, H. (1996). The transmembrane tyrosine phosphatase DLAR controls motor axon guidance in *Drosophila*. *Cell* **84**, 611–622.
- Laggerbauer, B., Ostareck, D., Keidel, E.-M., Ostareck-Lederer, A., and Fischer, U. (2001). Evidence that fragile X mental retardation protein is a negative regulator of translation. *Hum. Mol. Genet.* **10**, 329–338.
- Li, Z., Zhang, Y., Ku, L., Wilkinson, K.D., Warren, S.T., and Feng, Y. (2001). The fragile X mental retardation protein inhibits translation via interacting with mRNA. *Nucleic Acids Res.* **29**, 2276–2283.
- Luo, L. (2000). Rho GTPases in neuronal morphogenesis. *Nat. Rev. Neurosci.* **1**, 173–180.
- Luo, L. (2002). Actin cytoskeleton regulation in neuronal morphogenesis and structural plasticity. *Annu. Rev. Cell Dev. Biol.* **18**, 601–635.
- Luo, L., Liao, Y.J., Jan, L.Y., and Jan, Y.-N. (1994). Distinct morphogenetic functions of similar small GTPases: *Drosophila* Drac1 is involved in axonal outgrowth and myoblast fusion. *Genes Dev.* **8**, 1787–1802.
- Luo, L., Hensch, T.K., Ackerman, L., Barbel, S., Jan, L.Y., and Jan, Y.N. (1996). Differential effects of the Rac GTPase on Purkinje cell axons and dendritic trunks and spines. *Nature* **379**, 837–840.
- Martin, S.J., Grimwood, P.D., and Morris, R.G. (2000). Synaptic plasticity and memory: an evaluation of the hypothesis. *Annu. Rev. Neurosci.* **23**, 649–711.
- Meng, Y., Zhang, Y., Tregoubov, V., Janus, C., Cruz, L., Jackson, M., Lu, W.Y., MacDonald, J.F., Wang, J.Y., Falls, D.L., and Jia, Z.

- (2002). Abnormal spine morphology and enhanced LTP in LIMK-1 knockout mice. *Neuron* 35, 121–133.
- Miyashiro, K.Y., Beckel-Mitchener, A., Purk, T.P., Becker, K.G., Barret, T., Liu, L., Carbonetto, S., Weiler, I.J., Greenough, W.T., and Eberwine, J. (2003). RNA cargoes associating with FMRP reveal deficits in cellular functioning in *Fmr1* null mice. *Neuron* 37, 417–431.
- Morales, J., Hiesinger, P.R., Schroeder, A.J., Kume, K., Verstreken, P., Jackson, F.R., Nelson, D.L., and Hassan, B.A. (2002). *Drosophila* fragile X protein, DFXR, regulates neuronal morphology and function in the brain. *Neuron* 34, 961–972.
- Nakayama, A.Y., Harms, M.B., and Luo, L. (2000). Small GTPases Rac and Rho in the maintenance of dendritic spines and branches in hippocampal pyramidal neurons. *J. Neurosci.* 20, 5329–5338.
- Newsome, T.P., Schmidt, S., Dietzl, G., Keleman, K., Asling, B., Debant, A., and Dickson, B.J. (2000). Trio combines with dock to regulate Pak activity during photoreceptor axon pathfinding in *Drosophila*. *Cell* 101, 283–294.
- Ng, J., Nardine, T., Harms, M., Tzu, J., Goldstein, A., Sun, Y., Dietzl, G., Dickson, B.J., and Luo, L. (2002). Rac GTPases control axon growth, guidance and branching. *Nature* 416, 442–447.
- Nimchinsky, E.A., Oberlander, A.M., and Svoboda, K. (2001). Abnormal development of dendritic spines in FMR1 knock-out mice. *J. Neurosci.* 21, 5139–5146.
- Ramakers, G.J. (2002). Rho proteins, mental retardation and the cellular basis of cognition. *Trends Neurosci.* 25, 191–199.
- Rorth, P. (1996). A modular misexpression screen in *Drosophila* detecting tissue-specific phenotypes. *Proc. Natl. Acad. Sci. USA* 93, 12418–12422.
- Schaeffer, C., Bardoni, B., Mandel, J.L., Ehresmann, B., Ehresmann, C., and Moine, H. (2001). The Fragile X mental retardation protein interacts specifically with its own mRNA via a purine-quartet structure. *EMBO J.* 20, 4803–4813.
- Scheffzek, K., Ahmadian, M.R., and Wittinghofer, A. (1998). GTPase activating proteins: helping hands to complement an active site. *Trends Biochem. Sci.* 23, 257–262.
- Schenck, A., Bardoni, B., Moro, A., Bagni, C., and Mandel, J.L. (2001). A highly conserved protein family interacting with the fragile X mental retardation protein and displaying selective interactions with the FMRP related proteins FXR1P and FXR2P. *Proc. Natl. Acad. Sci. USA* 98, 8844–8849.
- Schenck, A., Van de Bor, V., Bardoni, B., and Giangrande, A. (2002). Novel features of dFMR1, the *Drosophila* orthologue of fragile X mental retardation protein. *Neurobiol. Dis.* 11, 53–63.
- Schmidt, A., and Hall, A. (2002). Guanine nucleotide exchange factors for Rho GTPases: turning on the switch. *Genes Dev.* 16, 1587–1609.
- Schuster, C.M., Davis, G.W., Fetter, R.D., and Goodman, C.S. (1996). Genetic dissection of structural and functional components of synaptic plasticity. I. Fasciclin II controls synaptic stabilization and growth. *Neuron* 17, 641–654.
- Steward, O., and Levy, W.B. (1982). Preferential localization of polyribosomes under the base of dendritic spines in granule cells of the dentate gyrus. *J. Neurosci.* 2, 284–291.
- Steward, O., and Schuman, E.M. (2001). Protein synthesis at synaptic sites on dendrites. *Annu. Rev. Neurosci.* 24, 299–325.
- Torre, E.R., and Steward, O. (1992). Demonstration of local protein synthesis within dendrites using a new cell culture system that permits the isolation of living axons and dendrites from their cell bodies. *J. Neurosci.* 12, 762–772.
- Wan, L., Dockendorff, T.C., Jongens, T.A., and Dreyfuss, G. (2000). Characterization of dFMR1, a *Drosophila* *Melanogaster* homolog of the fragile X mental retardation protein. *Mol. Cell. Biol.* 20, 8536–8547.
- Weiler, I.J., Irwin, S.A., Klintsova, A.Y., Spencer, C.M., Brazelton, A.D., Miyashiro, K., Comery, T.A., Patel, B., Eberwine, J., and Greenough, W.T. (1997). Fragile X mental retardation protein is translated near synapses in response to neurotransmitter activation. *Proc. Natl. Acad. Sci. USA* 94, 5395–5400.
- Zalfa, F., Giorgi, M., Primerano, B., Moro, A., Di Penta, A., Reis, S., Oostra, B., and Bagni, C. (2003). The fragile X syndrome protein FMRP associates with BC1 RNA and regulates the translation of specific mRNAs at synapses. *Cell* 112, 317–327.
- Zhang, Y.Q., Bailey, A.M., Matthiensi, H.J.G., Renden, R.B., Smith, M.A., Speese, S.D., Rubin, G.M., and Broadie, K. (2001). *Drosophila* fragile X-related gene regulates MAP1B homolog Futsch to control synaptic structure and function. *Cell* 107, 591–603.
- Zito, K., Parnas, D., Fetter, R.D., Isacoff, E.Y., and Goodman, C.S. (1999). Watching a synapse grow: noninvasive confocal imaging of synaptic growth in *Drosophila*. *Neuron* 22, 719–729.